

# Simulation of orbital decay of LEO satellites due to atmospheric drag during magnetic storms

Haiquan Yu

*Institute of Space Science and Application of Technology  
Harbin Institute of Technology  
Shenzhen, China  
20s058089@stu.hit.edu.cn*

Bo Chen\*

*Institute of Space Science and Application of Technology  
Harbin Institute of Technology  
Shenzhen, China  
hitchenbo@hit.edu.cn*

Boyi Wang

*Institute of Space Science and Application of Technology  
Harbin Institute of Technology  
Shenzhen, China  
wangboyi@hit.edu.cn*

Yanhua Pang

*Institute of Space Science and Application of Technology  
Harbin Institute of Technology  
Shenzhen, China  
gm.yanhuapang@gmail.com*

Xueshang Feng

*Institute of Space Science and Application of Technology  
Harbin Institute of Technology  
Shenzhen, China  
fengx@spaceweather.ac.cn*

Yang Zhao

*School of Computer Science and Technology  
Harbin Institute of Technology  
Shenzhen, China  
yang.zhao@hit.edu.cn*

**Abstract**—In order to understand the effect of geomagnetic activity on the orbits of LEO satellites with different orbital inclinations, we establish a model for the influence of atmospheric drag on the orbital decay of low Earth orbiting (LEO) satellites and simulate the orbital decay of seven LEO satellites during geomagnetic storms. In the simulation, the orbital inclinations of the seven LEO satellites are set to be 30°, 40°, 50°, 60°, 70°, 80°, and 88°, respectively. And the initial orbital heights are all 350km. The simulation results show that the seven LEO satellites are affected to different degrees during the geomagnetic storm, satellites with smaller orbital inclinations are more affected. The orbit of the Sat-A satellite with the smallest orbital inclination decreased by 1.794 km during the entire magnetic storm, while the orbit of the Sat-G satellite with the largest orbital inclination decreased by 1.530 km. We compare the local thermospheric atmosphere density on different satellite orbits and found that the atmosphere density on the orbits of LEO satellites with smaller orbital inclinations is greater, which means that LEO satellites with small orbital inclinations experience greater atmospheric drag. We deduce that the reason for this phenomenon is related to the density distribution of the thermospheric background atmosphere.

**Keywords**—atmospheric drag, thermospheric atmospheric density, LEO satellites, orbital inclination, geomagnetic storms, solar activity

## I. INTRODUCTION

In recent years, with the development of Internet technology and aerospace science and technology, the field of low Earth orbiting (LEO) satellite constellation has made leapfrog

development. Led by satellite constellation of Starlink and OneWeb, the number of low Earth orbiting satellite launches has increased rapidly. In low Earth orbit, atmospheric drag is the main factor causing the orbital attenuation of LEO satellites. It is well known that atmospheric drag is violently perturbed during geomagnetic storms. Therefore, studying the changes of LEO satellite orbits during geomagnetic storms is of great significance to satellite orbit determination, satellite orbit control and satellite collision probability calculation.

Atmospheric drag has an energy-dissipative nature, which will cause the satellite's orbit to decay continuously and the physical life of the satellite to be shortened [1]. Atmospheric drag perturbation is the main non-conservative force perturbation for LEO satellites (orbital altitude <800km). It is the main factor affecting the orbit change of LEO satellites. Without human intervention, atmospheric drag will cause LEO satellites to fall into the atmosphere prematurely. In addition, atmospheric drag disturbances make LEO satellites and space debris difficult to identify and track, and satellite lifetimes and collision probabilities are difficult to predict [2]. The local thermospheric atmospheric density variation in satellite orbits is the main factor causing the orbit attenuation of low-orbit satellites. The thermospheric atmosphere density is mainly affected by solar activity. Studies showed that the timescales of variations in thermospheric atmospheric density correlate with the timescales of solar activity cycles, flare events and geomagnetic storms [3].

During the geomagnetic quiet period, the solar EUV radiation is the main factor causing the change of the thermospheric

\*Corresponding author: Bo Chen.

This work is supported by Natural Science Foundation of Guangdong Province (No. 2022A151020113).

atmospheric density, which determines the basic structure of the background atmospheric density in the thermosphere. Cyclical variations in the density of the thermosphere atmosphere correspond to the solar rotation and solar activity cycles [4]. Studies showed that during the minimum to maximum years of a solar cycle, the solar EUV radiation flux and the temperature of the thermosphere increase by a factor of two, while the density of the thermosphere can increase by as much as 10 times [5]. However, Joule heating from strong geomagnetic disturbances is an important factor in causing changes in the atmospheric density of the thermosphere during short-term geomagnetic activity. During geomagnetic storms, when the Ap index increases from 4 to 80, the increase in Joule heating can reach 134% [6]. In addition, some scholars have analyzed the impact of geomagnetic storm events on satellite orbits based on measured satellite data (CHAMP, GRACE, SWARM, etc.) [7], [8] and numerical simulation data [9], [10], and deduced methods for calculating Precise Orbit Determination (POD) data [11].

Solar events including high-speed solar streams (HSS), coronal mass ejections (CMEs), solar flares and corotating interaction regions (CIRs) can affect the intensity and duration of geomagnetic storms [12]. The plasma carried by CME and CIR interacts with the Earth's magnetosphere, causing disturbance of the Earth's magnetic field and forming global-scale geomagnetic storms [13]. Some investigation show that CIR-induced geomagnetic storms may have much larger changes in thermospheric atmospheric density and satellite orbit attenuation than CME-induced geomagnetic storms. CME-induced geomagnetic storms cause larger thermospheric atmospheric density perturbations that lead to larger orbital decay rates for satellites, but shorter durations. Although CIR-induced geomagnetic storms cause less perturbation in thermospheric atmosphere density, duration of CIR phase is longer [14]. The effects of CIR and HSS on changes in thermospheric atmospheric density and satellite orbits during the decay phase of the solar cycle are important because CIR and HSS are the main drivers of induced geomagnetic storms during this phase [13]–[15].

To sum up, many scholars have analyzed the influence of solar activity and geomagnetic activity on satellite orbits in the form of measured satellite data or simulated data. However, there are few studies on the influence of atmospheric drag on the orbit attenuation of LEO satellites with different orbital inclinations during geomagnetic storms. As the number of orbits and satellites occupied by low-orbit constellations increases, the probability of collision between satellites will increase, and the orbital changes of a single satellite may affect the function of the entire satellite constellation. It is of great significance to study the satellite orbit changes with different orbit inclinations for the collision warning and life prediction of low-orbit constellation satellites. In addition, our research provides a reference for calculating the collision probability of LEO satellites in different orbits during magnetic storms, and for orbit prediction and orbit adjustment of LEO satellites.

## II. MODELING LEO SATELLITE ORBITAL DECAY

In order to complete the simulation experiment, we need to establish a satellite orbit dynamics model under the action of atmospheric drag. The process of numerical simulation is shown in Fig. 1. In this work, our model mainly consists of three parts: orbital perturbation module, atmospheric model module and numerical integration module. Inputs to the model: simulation time, geomagnetic index, F10.7 index, satellite surface-to-mass ratio, drag coefficient and satellite initial orbital elements. The output of the model: semi-major axis, semi-major axis decay rate, atmospheric density change, aerodynamic drag on LEO satellites, etc.

### A. Satellite orbit perturbation

The perturbations of satellites in orbit include: perturbations caused by the non-sphericity of the earth and uneven mass, atmospheric resistance perturbations of the upper atmosphere, solar light pressure perturbations, sun-moon gravitational perturbations, tidal force perturbations, and earth radiation pressures perturbation etc. Under the action of the perturbation force, the orbital parameters of the satellite are constantly changing and no longer follow the two-body orbit. The main perturbations of LEO satellites are the Earth's aspherical perturbation and atmospheric drag perturbation. Therefore, only these two main perturbing forces are considered in the modeling.

The equation of motion of the satellite in the earth's gravitational field [16]:

$$\ddot{\mathbf{r}} = -\frac{\mu}{r^3} \mathbf{r} + \mathbf{a} \quad (1)$$

where  $\mathbf{r}$  is the position vector of the satellite,  $\mathbf{a}$  is the acceleration of various perturbation forces and  $\mu$  is the Earth's gravitational constant.

For atmospheric drag perturbation, the drag acceleration caused by the atmosphere to LEO satellites [17]:

$$\mathbf{a}_D = -\frac{1}{2} C_D \frac{A}{m} \rho v \mathbf{v} \quad (2)$$

$C_D$ ,  $A$ ,  $m$ ,  $\mathbf{v}$ ,  $v$ ,  $\rho$  represent the drag coefficient, Cross-section of the satellite in the direction of velocity, the satellite mass, the satellite motion velocity vector, the satellite motion velocity scalar, and the atmospheric density, respectively. The drag acceleration of a satellite is related to its drag coefficient, surface-to-mass ratio, atmospheric density, and velocity.

### B. Atmospheric Model and Numerical integration methods

In this work, the atmospheric model used in our modeling is the NRLMSISE-00 Thermospheric Neutral Atmosphere Empirical Model [18]. There are two types of methods for solving differential equations, one is the analytical method and the other is the numerical integration method. For complex orbital dynamics perturbation equations, it is difficult to solve the derivation by analytical methods, and the accuracy requirements cannot be guaranteed [17], [19]. Therefore, we use the Runge-Kutta numerical integration method to solve the orbital perturbation equation.

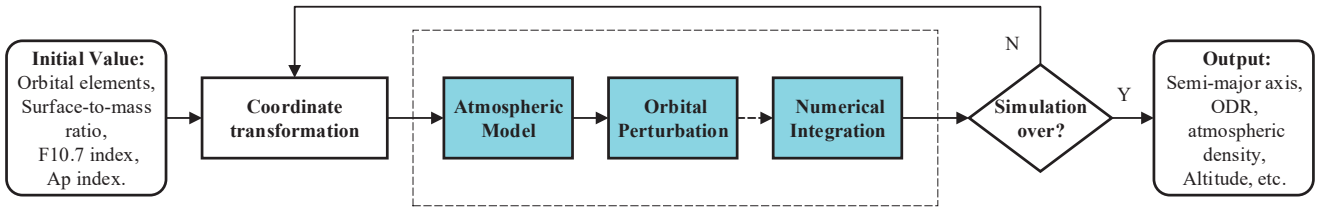


Fig. 1. The process of numerical simulation.

### III. METHOD AND SCOPE

In order to study the orbital changes of LEO satellites with different orbital inclinations during geomagnetic storms, we need to find a classical geomagnetic storm event and set appropriate orbital parameters of LEO satellites for simulation experiments.

#### A. Geomagnetic storm event selection

Thermospheric atmospheric density is affected by both solar radiation and geomagnetic storms. In order to control variables as much as possible and analyze the impact of geomagnetic storms on satellite orbits, we should select magnetic storm events with small changes in solar radiation flux and relatively large intensity of magnetic storms to highlight the impact of geomagnetic activity on satellite orbit changes. Based on the above principles, the geomagnetic storm event on March 16, 2015 was selected for simulation experiments. During this magnetic storm, the F10.7 index of solar radiation flux did not change much, and the minimum geomagnetic index reached -223nT, which belonged to the type of super magnetic storm. The space weather parameters from March 16, 2015 to March 20, 2015 are shown in Fig. 2. It can be seen that the F10.7 index remains stable throughout the storm. The day before the occurrence of the magnetic storm, the speed of the solar wind increased slowly, and other space weather parameters fluctuated slightly, which was not enough to form a global geomagnetic disturbance. During March 17, a brief southward component of the interplanetary magnetic field(IMF) appeared, at which time there was an obvious peak in the solar wind dynamic pressure, which promoted the entry of solar particles into the Earth's magnetosphere and formed a geomagnetic disturbance. After that, a persistent north component of the interplanetary magnetic field appears, and the northward interplanetary magnetic field will have magnetic reconnection with the Earth's magnetosphere, causing geomagnetic disturbance. It can be seen from the geomagnetic index that a strong geomagnetic storm occurred after March 17.

#### B. Satellite orbit parameter settings

To study the effect of geomagnetic storms on the orbital attenuation of LEO satellites with different orbital inclinations, we simulated the attenuation of 7 LEO satellites (Sat-A, Sat-B,

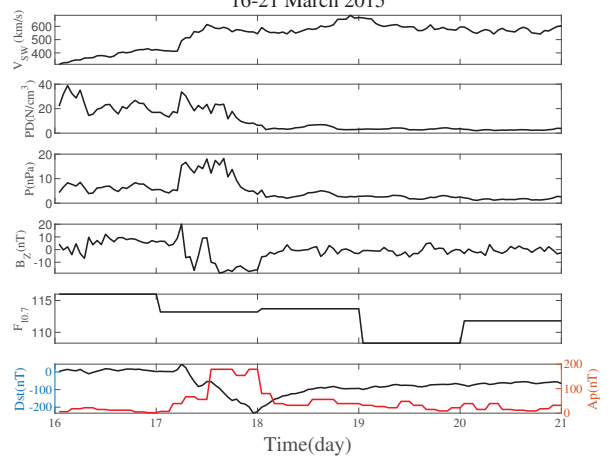


Fig. 2. Solar wind speed ( $V_{SW}$ ), proton density(PD), solar wind dynamic pressure(P),  $B_z$  component of the interplanetary magnetic field, F10.7 index, Dst index and Ap index during 16-21 March, 2015.

Sat-C, Sat-D, Sat-E, Sat-F, Sat-G) with different orbital inclinations during geomagnetic storms. To control for variables, we make the surface-to-mass ratio and drag coefficient the same for each LEO satellite, and the satellite orbital altitude is 350km. The parameters of the LEO satellites are given in Table I.

TABLE I  
INITIALIZATION PARAMETERS OF THE LEO SATELLITES

	H(km)	Inclination(°)	$A/m(m^2/kg)$	$C_d$
Sat-A	350	30	0.008461	2.2
Sat-B	350	40	0.008461	2.2
Sat-C	350	50	0.008461	2.2
Sat-D	350	60	0.008461	2.2
Sat-E	350	70	0.008461	2.2
Sat-F	350	80	0.008461	2.2
Sat-G	350	88	0.008461	2.2

### IV. RESULT AND DISCUSSION

#### A. Effects of Magnetic Storms on LEO satellites

After a magnetic storm, both the density and temperature of the thermospheric atmosphere are perturbed. The simulation

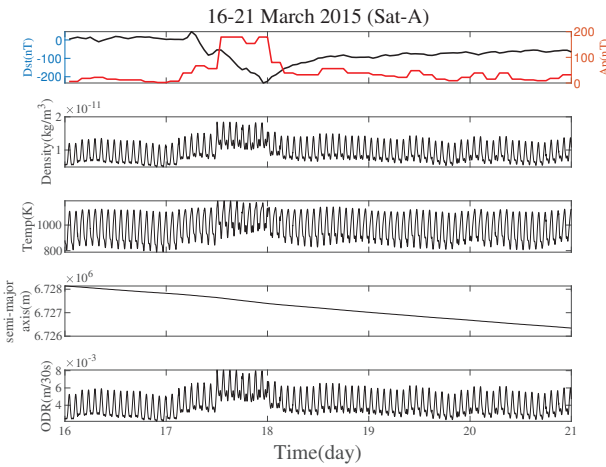


Fig. 3. Dst index and Ap index, Thermospheric Atmosphere Density and Temperature, orbital semi-major axis and orbital decay rate (ODR) for Sat-A during 16-21 March, 2015.

results of the Sat-A satellite during March 16-21, 2015 are shown in Fig. 3, which shows the orbital semi-major axis variation of the Sat-A satellite, the orbital decay rate, and the thermospheric atmosphere density and temperature on the satellite orbit during the magnetic storm. On March 16, the local thermospheric atmospheric density and atmospheric temperature in the satellite orbit remained relatively stable. After the geomagnetic storm occurred on March 17, the density of the thermospheric atmosphere gradually increased, reaching a peak around 12:00. The orbital decay rate varies with the density of the atmosphere in the thermosphere. It can be seen from Fig. 2 that the intensity of the geomagnetic storm was the greatest on March 17, and both the orbital decay rate and the decay of the semi-major axis of the orbit reached the maximum on this day.

#### B. Comparison of the orbital decay during magnetic storm

In order to study the orbital attenuation of LEO satellites with different orbital inclinations during geomagnetic storms, we compared the semi-major axis changes of different satellites during March 16-20, 2015, as shown in Fig. 4. It is obvious that the smaller the orbital inclination, the greater the attenuation of the semi-major axis of the LEO satellite. The daily orbital attenuation and total attenuation of the seven LEO satellites are summarized in Table II. The visualization of the orbital attenuation of each satellite is shown in Fig. 5. It can be seen that the orbital attenuation of each satellite is the largest on the 17th. Among them, the Sat-A satellite has the largest orbital attenuation, which is 416m/day. The Sat-G satellite has the smallest orbital attenuation, which is 373m/day. During the entire magnetic storm, the total orbital attenuation of the Sat-A satellite was the largest (1794m), and the Sat-G satellite was the smallest (1530m).

To explore the difference in the orbital attenuation of satellites with different orbital inclinations, we compared the local

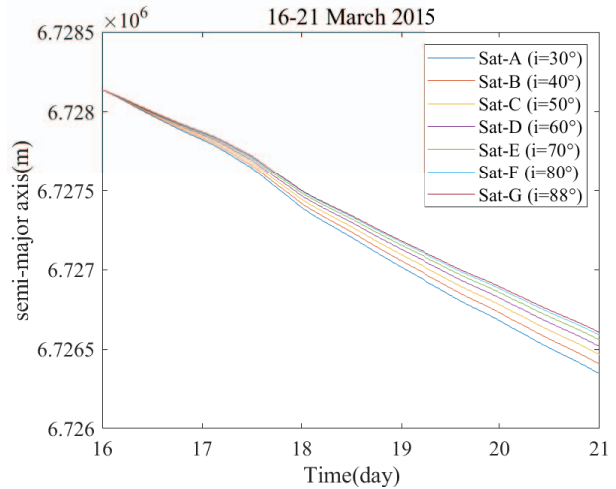


Fig. 4. Orbital semi-major axis variation of Sat-A, Sat-B, Sat-C, Sat-D, Sat-E, Sat-F, Sat-G during 16-20 March, 2015.

TABLE II  
ORBITAL DECAY FOR MARCH 16-20

Satellite Name	Orbital Decay(m)					
	16,Mar	17,Mar	18,Mar	19,Mar	20,Mar	Total
Sat-A	312	432	376	338	336	1794
Sat-B	302	416	363	326	325	1732
Sat-C	291	401	350	316	314	1672
Sat-D	280	389	339	307	304	1619
Sat-E	271	380	330	299	297	1578
Sat-F	265	376	323	292	291	1547
Sat-G	262	373	319	289	286	1530

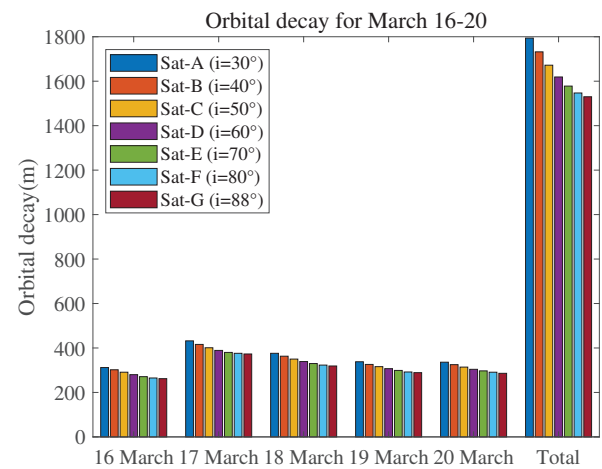


Fig. 5. Orbital decay of Sat-A, Sat-B, Sat-C, Sat-D, Sat-E, Sat-F, Sat-G during 16-20 March, 2015.

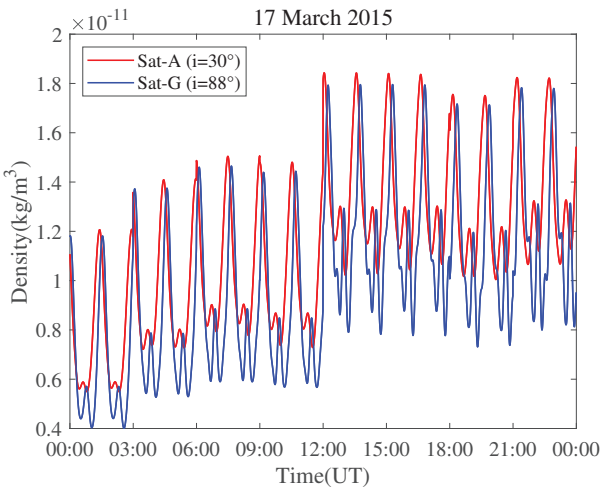


Fig. 6. Comparison of the density of the thermospheric atmosphere on the Sat-A and Sat-G orbits on March 17, 2015

thermospheric atmosphere densities on the satellite orbits of Sat-A and Sat-G on March 17, as shown in Fig. 6. Obviously, the Sat-A experienced greater atmospheric drag than the Sat-G. This difference may be due to the fact that satellites with smaller orbital inclinations spend longer traversing times at low and middle latitudes than satellites with larger orbital inclinations. The thermospheric atmosphere is denser at mid-low latitudes than at high latitudes, so satellites with smaller orbital inclinations experience greater orbital attenuation during magnetic storms.

## V. CONCLUSION

The simulation results show that LEO satellites with different orbital inclinations are all affected by the geomagnetic storm from March 16 to 21, 2015, and each LEO satellite has the largest orbital attenuation on the day of the strongest magnetic storm. The Sat-A satellite with the smallest orbital inclination is most affected by the geomagnetic storm. The average orbital decay rate of the Sat-A satellite over the entire storm period is 358.8 m/day, while that of Sat-G is 306 m/day. Through comparative analysis, we found that the LEO satellite with a smaller orbital inclination has a larger local thermospheric atmosphere density when orbiting, which causes satellite to experience more atmospheric drag. We speculate that the reason for this phenomenon may be related to the structure of the background atmosphere of the thermosphere. The orbital planes of LEO satellites with smaller orbital inclinations are located at lower latitudes. Due to the thermosphere is denser in the mid-low latitudes than in the high latitudes, LEO satellites with smaller orbital inclinations are more affected by atmospheric drag during magnetic storms. Our research could be useful for calculating the collision probability of LEO satellites in different orbits during the magnetic storm, and provides a reference for the orbit prediction and orbit adjustment of LEO satellites.

## ACKNOWLEDGMENT

We greatly appreciate the use of space weather data from OMNIWeb service of NASA's Goddard Space Flight Center.

## REFERENCES

- [1] E. Doornbos and H. Klinkrad, "Modelling of space weather effects on satellite drag," *Advances in Space Research*, vol. 37, no. 6, pp. 1229–1239, 2006.
- [2] V. U. Nwankwo, S. K. Chakrabarti, and R. S. Weigel, "Effects of plasma drag on low earth orbiting satellites due to solar forcing induced perturbations and heating," *Advances in Space Research*, vol. 56, no. 1, pp. 47–56, 2015.
- [3] I. Kutiev, I. Tsagouri, L. Perrone, D. Pancheva, P. Mukhtarov, A. Mikhailov, J. Lastovicka, N. Jakowski, D. Buresova, E. Blanch *et al.*, "Solar activity impact on the earth's upper atmosphere," *Journal of Space Weather and Space Climate*, vol. 3, p. A06, 2013.
- [4] G. Wilson, D. Weimer, J. Wise, and F. Marcos, "Response of the thermosphere to joule heating and particle precipitation," *Journal of Geophysical Research: Space Physics*, vol. 111, no. A10, 2006.
- [5] J. Emmert and J. Picone, "Climatology of globally averaged thermospheric mass density," *Journal of Geophysical Research: Space Physics*, vol. 115, no. A9, 2010.
- [6] K.-H. Kim, Y.-J. Moon, K.-S. Cho, H.-D. Kim, and J.-Y. Park, "Atmospheric drag effects on the kompsat-1 satellite during geomagnetic superstorms," *Earth, planets and space*, vol. 58, no. 6, pp. e25–e28, 2006.
- [7] A. Calabia and S. Jin, "Thermospheric density estimation and responses to the march 2013 geomagnetic storm from grace gps-determined precise orbits," *Journal of Atmospheric and Solar-Terrestrial Physics*, vol. 154, pp. 167–179, 2017.
- [8] K. Zhang, X. Li, C. Xiong, X. Meng, X. Li, Y. Yuan, and X. Zhang, "The influence of geomagnetic storm of 7–8 september 2017 on the swarm precise orbit determination," *Journal of Geophysical Research: Space Physics*, vol. 124, no. 8, pp. 6971–6984, 2019.
- [9] F. YIN, S.-Y. MA, J. LI, D.-H. FENG, X.-J. WANG, and Y.-L. ZHOU, "Simulation of orbit decay for leo satellites caused by atmospheric drag," *Chinese Journal of Geophysics*, vol. 56, no. 12, pp. 3980–3987, 2013.
- [10] V. U. Nwankwo, W. Denig, S. K. Chakrabarti, M. P. Ajakaiye, J. Fatokun, A. W. Akanni, J.-P. Raulin, E. Correia, and J. E. Enoh, "Atmospheric drag effects on modelled leo satellites during the july 2000 bastille day event in contrast to an interval of geomagnetically quiet conditions," *Annales Geophysicae Discussions*, vol. 2020, pp. 1–24, 2020.
- [11] R. Li and J. Lei, "The determination of satellite orbital decay from pod data during geomagnetic storms," *Space Weather*, vol. 19, no. 4, p. e2020SW002664, 2021.
- [12] F. Delefie, K. Doerksen, C. Briand, M. A. Sammuneh, and L. Sagnières, "Atmospheric density variations and orbit perturbations in relation to isolated solar x-flare events," in *EGU General Assembly Conference Abstracts*, in: *EGU General Assembly Conference Abstracts*, 2019, p. 15338.
- [13] A. Burns, S. Solomon, L. Qian, W. Wang, B. Emery, M. Wiltberger, and D. Weimer, "The effects of corotating interaction region/high speed stream storms on the thermosphere and ionosphere during the last solar minimum," *Journal of Atmospheric and Solar-Terrestrial Physics*, vol. 83, pp. 79–87, 2012.
- [14] G.-m. Chen, J. Xu, W. Wang, J. Lei, and A. G. Burns, "A comparison of the effects of cir-and cme-induced geomagnetic activity on thermospheric densities and spacecraft orbits: Case studies," *Journal of Geophysical Research: Space Physics*, vol. 117, no. A8, 2012.
- [15] V. U. Nwankwo and S. K. Chakrabarti, "Theoretical model of drag force impact on a model international space station satellite due to solar activity," *TRANSACTIONS OF THE JAPAN SOCIETY FOR AERONAUTICAL AND SPACE SCIENCES, AEROSPACE TECHNOLOGY JAPAN*, vol. 12, pp. 47–53, 2014.
- [16] S. Khodairy, M. Sharaf, M. Awad, R. A. Hamed, and M. Hussein, "Impact of solar activity on low earth orbiting satellites," in *Journal of Physics: Conference Series*, vol. 1523, no. 1. IOP Publishing, 2020, p. 012010.

- [17] E. Doornbos, M. Förster, B. Fritsche, T. van Helleputte, J. van den IJssel, G. Koppenwallner, H. Lühr, D. Rees, P. Visser, and M. Kern, “Air density models derived from multi-satellite drag observations,” in *Proceedings of ESAs Second Swarm International Science Meeting, Potsdam*. 24, vol. 26, 2009.
- [18] J. Picone, A. Hedin, D. P. Drob, and A. Aikin, “Nrlmsise-00 empirical model of the atmosphere: Statistical comparisons and scientific issues,” *Journal of Geophysical Research: Space Physics*, vol. 107, no. A12, pp. SIA-15, 2002.
- [19] O. Montenbruck, E. Gill, and F. Lutze, “Satellite orbits: models, methods, and applications,” *Appl. Mech. Rev.*, vol. 55, no. 2, pp. B27–B28, 2002.